molecular informatics
models – molecules – systems

Accepted Article

Title: Aporphinoid alkaloids derivatives as selective cholinesterases inhibitors: biological evaluation and docking study

Authors: Lucas Joel Gutierrez, Valeria Cavallaro, Ana Paula Murray, and Carlos Pungitore

To be cited as: *Mol. Inf.* 10.1002/minf.201900125

Link to VoR: http://dx.doi.org/10.1002/minf.201900125

molecular informatics

DOI: 10.1002/minf.200((full DOI will be filled in by the editorial staff))

Aporphinoid alkaloids derivatives as selective cholinesterases inhibitors: biological evaluation and docking study

Valeria Cavallaro, [a], Ana Paula Murray, [a] Carlos Rodolfo Pungitore, [b] and Lucas Joel Gutiérrez *[c]

Dedication In memory of Dr. Matías Nieto of Facultad de Química, Bioquímica y Farmacia, Universidad Nacional de San Luis, San Luis, Argentina.

Abstract: Alzheimer´s dementia is a neurodegenerative disease that affects the elderly population and causes memory impairment and cognitive deficit. Manifestation of this disease is associated to acetylcholine decrease; thus, Cholinesterase inhibition is the main therapeutic strategy for the treatment of Alzheimer's disease.
In the present study, a series of aporphinoid alkaloids were tested as potential acetylcholinesterase (AChE) and butyrylcholinesterase (BChE) inhibitors *in vitro*. Alkaloids liriodenine (**3**) and cassythicine (**10**) were the best inhibitors of both cholinesterases with IC_{50} values lower than 10 µM. In addition, these alkaloids demonstrated better inhibition of BChE than reference drug galantamine.
In addition, some alkaloids showed selective inhibition. Laurotetatine clorhydrate (**13**) selectively inhibit AChE over BChE. On the contrary, pachyconfine (**7**) interacted more efficiently with BChE active site.
Molecular modelling studies were performed in order to illustrate key interactions between most active compounds and the enzymes and to explain their selectivity. These studies reveal that the benzodioxole moiety exhibits strong interactions due to hydrogen bonds that form with the Glu201 (AChE) and Tyr440 (BChE) residues, which is reflected in the IC_{50} values.

Keywords: Acetylcholinesterase; Aporphinoid; Butyrylcholinesterase; Molecular modelling.

1 Introduction

Alzheimer's disease (AD) is one of the most common neurodegenerative disorder affecting approximately 47 million people worldwide. With the progressive aging of the population, AD has become a serious medical problem in modern society. The complexity and still unclear pathology of this disease makes treatment difficult. [1]

One of the most widely accepted explanations of AD development is the cholinergic hypothesis, which offers clear directions for treatment strategies. [2] Cholinesterases (ChE) are a family of enzymes that mainly catalyze the hydrolysis of the neurotransmitter acetylcholine (ACh) restoring the cholinergic pathway at the end of the nerve transmission in the central nervous system. There are two major forms of cholinesterases in vertebrates: acetyl and butyrylcholinesterase (AChE and BChE). While AChE prevails in a healthy brain, BChE activity increases in patients with AD. Thus, AChE and BChE inhibition have been documented as critical targets for the effective management of AD. [3-5] Drugs acting as cholinesterase inhibitors (ChEI) have shown several benefits including improvement of brain ACh levels resulting in an enhanced cholinergic transmission. Nowadays ChEI represent the main treatment to ameliorate the cognitive and behavioral dysfunctions associated with AD. [6,7]

Aporphinoids are an important class of alkaloids widely distributed in the plant kingdom. These natural compounds have been shown to exhibit an important spectrum of pharmacological activities as an antimicrobial [8], antitumor [9], and antifungal, [10] among others. Even though, potent cholinesterase inhibition has been reported for members of this alkaloid subgroup little is known on their mode of inhibition. [11-13]

Continuing our studies on cholinesterase inhibitors from natural sources in this work we evaluate set of thirteen aporphinoid alkaloids as AChE and BChE inhibitors *in vitro*. In addition, the key binding interactions between these compounds and the enzymes are studied by docking calculation with hybrid (Quantum Mechanics/Molecular Mechanics) QM/MM calculations (ONIOM). Finally, a Quantum Theory of Atoms in Molecules (QTAIM) study is performed in order to understand the selectivity of these compounds

2 Materials and Methods

2.1 Aporphinoid alkaloids

[a] *INQUISUR-CONICET, Departamento de Química, Universidad Nacional del Sur, Av. Alem 1253, 8000 Bahía Blanca, Argentina.*

[b] *INTEQUI-CONICET, Departamento de Química, Universidad Nacional de San Luis, Almirante Brown 907, 5700, San Luis, Argentina.*

[c] *IMIBIO-SL CONICET, Facultad de Química, Bioquímica y Farmacia, Universidad Nacional de San Luis, República de Argentina, San Luis, Argentina. Ejército de los Andes 950, 5700 San Luis, Argentina*
**e-mail: lucasg@unsl.edu.ar*

Supporting Information for this article is available on the WWW under www.molinf.com

cholinesterases inhibitors

Thirteen alkaloids were isolated in previous research works from different plants species like *Rollinia marginata* (Schlecht) from Chaco, Argentina; *Enantia pilosa* (Exell); *Xylopia lemúrica* (Diels) *Pachypodanthium staudtii* and *Guatteria psilopus* from Republic of Congo, Africa [14] using techniques as described in [15]. Alkaloids were kindly granted by Department of Chemistry from South Paris University, France, through Dr. Matıas Nieto and Dr. Carlos R. Pungitore. Scheme 1 shows the chemical structure of the tested alkaloids.

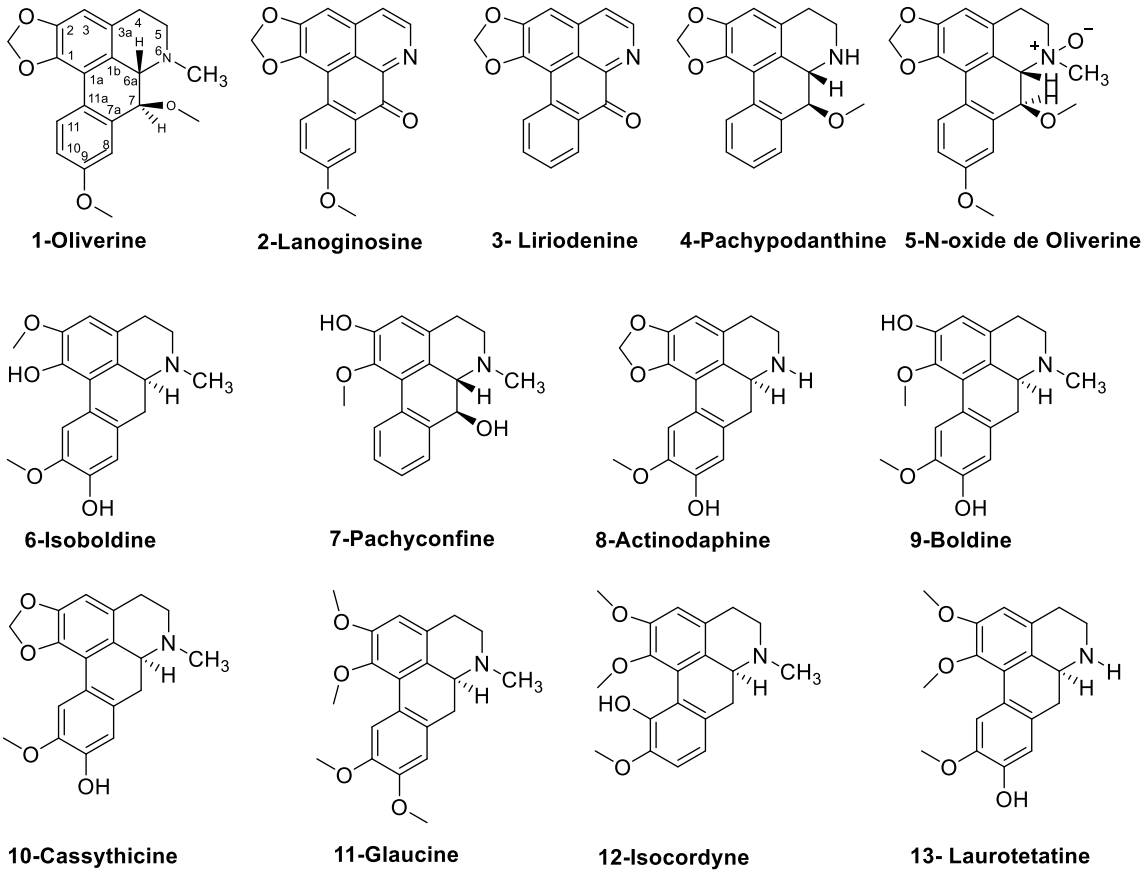

Scheme 1. Structures of compounds employed in this study.

2.2 Cholinesterase inhibition assay

Electric eel (*Torpedo californica*) AChE and horse serum BChE were used as cholinesterase source. AChE and BChE inhibitory activity were measured in vitro by the spectrophotometric method developed by Ellman with slight modifications. [16] The lyophilized enzymes, 500 U AChE/ 300 U BChE, were dissolved in buffer A (8 mM K_2HPO_4, 2.3 mM NaH_2PO_4) to obtain 5/3 U/mL stock solutions. Further enzyme dilutions were carried out with buffer B (8 mM K_2HPO_4, 2.3 mM NaH_2PO_4, 0.15 M NaCl, 0.05% Tween 20, pH 7.6) to produce 0.126/0.06 U/mL enzyme solution. Samples were dissolved in buffer B. Compounds required 2.5% of MeOH as cosolvent. Enzyme solution (300 µL) and 300 µL of sample solution were mixed in a test tube and incubated for 60/120 min at room temperature. The reaction was started by adding 600 µL of the substrate solution (0.5 mM DTNB, 0.6 mM ATCI, 0.1 M Na_2HPO_4, pH 7.5). The absorbance was read at 405 nm for 120 s at 27 °C. Enzyme activity was calculated by comparing reaction rates for the sample to the blank. All the reactions were performed in triplicate. IC_{50} values (the inhibitor concentration required for 50% inhibition of the enzyme) were determined with GraphPad Prism5. Galanthamine was used as the reference AChE/BChE inhibitor.

2.3 Docking Calculations

The docking simulations were carried out using of AutoDock 4.2. [17] The crystal structures for the AChE and BChE were obtained from the Protein Data Bank. In order to remove the bad contacts from the X-ray structure, each receptor molecule was subjected to 1000 steps of energy minimization using the Amber16 program.[18] Then, the compounds were docked in each enzyme. In docking experiments the following parameters were used: the initial population of trial ligands was constituted by 250 individuals; the maximum number of generations was set to 270000. The maximum number of energy evaluations was 10.0×10^6. All other run parameters were maintained at their default setting. The resulting docked conformations were clustered into families by the backbone Root Mean Square Deviation.

2.4 Refinement of the anchoring and QTAIM analysis

After the docking calculations, leading lowest energy structures were optimized at M06-2X/631G(d) level using QM/MM calculations. The inhibitors and the side chains of the residues that have at least one heavy atom within 4 Å from the ligand molecule (first shell residues) were incorporated into the high-level QM layer using the M06-2X/631G(d) method.

The chosen cut-off value has resulted from a compromise between computational cost and efficiency. [19] The remainder of the system was included in the low-level MM layer using the AMBER force field. The MM parameters absent in the standard AMBER force field were included from the generalized amber force field (GAFF). [20] These calculations were carried out employing the Gaussian 09 package. [21] Then, the optimized geometry for each inhibitor-Cholinesterase complex was used as input for Quantum Theory of Atoms in Molecules (QTAIM) analysis, [22] which was carried out using the Multiwfn software, [23] employing the wave functions generated at the M06-2X/6-31G(d) level.

3 Results and Discussion

3.1 In vitro AChE and BChE inhibitory activities

Thirteen structurally related alkaloids were evaluated as cholinesterase inhibitors by the Ellman's method. BChE inhibition was tested for all the alkaloids while AChE inhibition was determined for those that had not been reported previously (**1**, **2**, **4**, **5**, **7**, **10-12**). For compounds **3**, **6**, **8**, **9**, and **13,** which have shown AChE inhibition in the past, their reported values of IC_{50} were taken into account for comparison purposes. [11,24] The IC_{50} values for enzyme inhibition, along with their standard deviations, and the selectivity index for the inhibition of AChE over BChE are summarized in **Table 1**. Compounds with IC_{50} values over 250 µM were considered inactive in this work. The alkaloid galanthamine, an FDA-approved drug for the treatment of AD, was used as reference AChE and BChE inhibitor.

All tested alkaloids showed inhibitory activity for at least one of the enzymes in the micromolar range. Alkaloid **13** elicited the most potent activity against AChE with a reported IC_{50} value of 3.2 µM [Mollataghi, 2012], although it showed a weak BChE inhibition (IC_{50}= 193.1 ± 2.9 µM). Compound **3**, liriodenine, exhibited strong inhibition on both AChE and BChE activities and showed poor selectivity with IC_{50} values of 3.5 µM [11] and 3.2 ± 0.1 µM, respectively.

As can be concluded from the IC_{50} values in Table 1, laurotetatine clorhydrate (**13**) was the most selective inhibitor of AChE over BChE. On the other hand, pachyconfine (**7**) seemed to interact better with BChE active site.

Alkaloids **1**, **2** and **11** demonstrated no inhibition for BChE while only compound **12** resulted inactive for AChE.

3.2 Molecular modelling

In order to better understand the above described experimental results, a molecular modelling study was conducted by using combined simulation techniques. This study was carried out in several stages. First, five alkaloids were selected and subjected a docking study in order to find the binding mode in the AChE and BChE enzyme. Second, the complexes obtained in the first stage were subjected to hybrid QM/MM calculations (ONIOM), where the geometries of the residues of binding site and the inhibitor were optimized at quantum level. Finally, to better appreciate the molecular interactions involved in the different Ligand-Receptor complexes and to understand the selectivity of these compounds, a QTAIM study was performed. The main goal of this study was to determine the possible mechanism of action of the compounds reported here and explain the selectivity of these inhibitors.

In order to validate the parameters employed in the docking calculations, we attempted to reproduce the binding mode of complexes AChE-Ganlantamine (pdbcode: 4EY6) [25] and BChE-tacrine (pdbcode: 4BDS).[26]

Table 1. Cholinesterase inhibitory activities of alkaloids expressed as IC_{50} (µM).

Alkaloid	IC_{50} (µM)		Selectivity index[a]
	AChE	BChE	
1	50.3 ± 1.4	> 250	> 5
2	176.5 ± 1.8	> 250	> 1.4
3	3.5*	3.2 ± 0.1	0.9
4	83.6 ± 2.5	20.7 ± 1.0	0.2
5	202.8 ± 3.7	74.3 ± 1.2	0.4
6	9.4*	152.3 ± 2.0	16.2
7	213.0 ± 3,2	16.5 ± 0.3	0.01
8	47[#]	14.5 ± 0.6	0.3
9	8.5*	102.2 ± 1.4	12.0
10	5.5 ± 0.2	9.8 ± 0.2	1.8
11	214.9 ± 2.6	> 250	> 1.2
12	>250	86.8 ± 3.4	> 0.3
13	3.2*	193.1 ± 2.9	60.3
Ref[b]	0.8 ± 0.01	23.8 ± 1.1	29.8

[a]Selectivity index = IC_{50} (BChE)/IC_{50} (AChE).
[b]Reference inhibitor.
*Reference [11]
[#]Reference [24]

The lowest energy conformations obtained from the docking calculations for the AChE-Ganlantamine and BChE-tacrine complexes presents the RMSD values 0.24 and 0.37 Å for the complex AChE-Ganlantamina and BChE-tacrine, respectively. In principle, these results suggest that the parameters used in the docking calculations were adequate for this study.

3.3 Binding mode selections

Figure 1 shows a summary of the molecular docking results, here are plotted the number of conformations of each cluster for all compounds. It should be noted, that the docking calculations suggest several modes of binding for each compound and the binding energies between the clusters are similar, thus, the leader of the most populated cluster was selected for further study. In the AChE system, the leader of cluster 2, 2, 2, 1 and 1 were selected for the compound **3**, **4, 7, 8** and **10** respectively, while in the BChE complex the leader of cluster 1, 1, 1, 1 and 1 was selected for the compounds **3**, **4, 7, 8** and **10** respectively.

It must be highlighted that the binding mode of the conformations chosen as the most favorable for AchE inhibition are similar to that of galantamine. This is because they are structurally similar. The compounds reported here, have three groups (HBA, HBD and HBA) separated by 6.2, 6.6 and 7.3 Å, while galantamine has the like group separated by 6.5, 5.4 and 6.8 Å respectively (**Figure 2**).

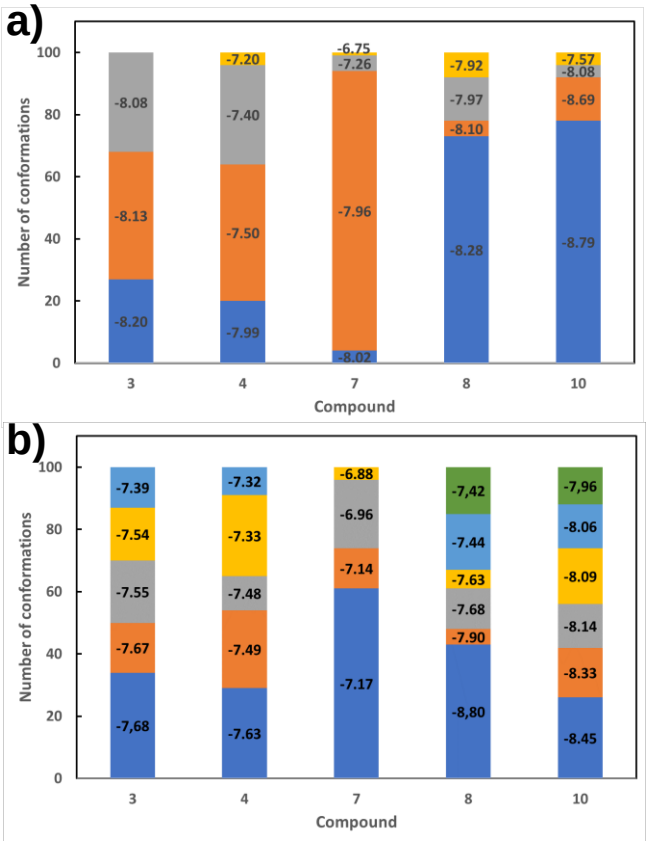

Figure 1. Summary of molecular docking calculations for a) AChE-inhibitor complex and b) BChE-inhibitor complex. Bars indicate the number of conformations that form each cluster. In black color the free energy of union of the leader of each cluster are shown.

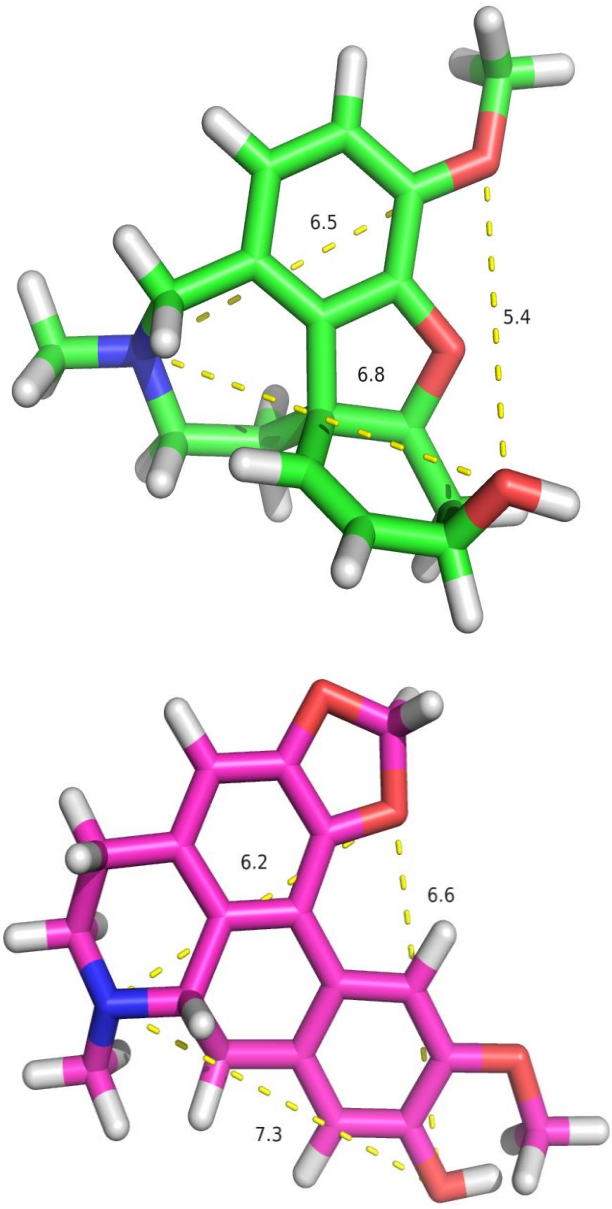

Figure 2. Structural comparison between galantamine (a) and compound **8** (b). The triangle in dot lines shows the interatomic distances between the main functional groups.

Thus, these compounds present hydrophobic contacts and aromatic interactions mainly with the Trp85, Gly120, Phe296 and Phe337, while the H-bond acceptor group forming a hydrogen bond with Ser202 and the H-bond donor group presents a hydrogen bond with Tyr132. The last one, in the galantamine case this hydrogen bond is with Glu201, due to the group separation is less.

For the BChE complexes, we can see that the favorable conformations chosen for each inhibitor have a binding mode like tacrine, although these do not present a marked structural similarity. These compounds are joined to BChE mainly by two hydrogen bonds between for the benzodioxolo moiety and residues Tyr332 and Tyr440. In addition, the compounds **3**, **4** and **7** presents

other anchorage point forming a strong hydrogen bond with Thr120. On the other hand, compounds **8** and **10** have a strong hydrogen bond with Thr120 but, through the hydroxyl moiety.

3.4 QTAIM analysis

The QTAIM analysis is an important tool in the study of ligand-receptor interactions because the values of the electronic density at a critical point (CPB) indicate the strength of the interactions. In addition, this information allows us to visualize which portion of the ligand presents a greater contribution to the binding, which makes it particularly useful in analysis, design and optimization of ligand molecules. However, for the QTAIM analysis to be reliable, good geometry is needed. For this reason, the structures obtained from the molecular docking were optimized at M06-2X/631G(d) level using QM-MM calculations as described in section **2.4**.
Figure 3, show in bars the sum of the charge density values at the intermolecular bond critical points for the non-covalent interactions for the five inhibitors with the AChE and BChE enzyme. This plot shows that the inhibitors bind more strongly to BChE than to AChE. This means that the selectivity could be explained through the interactions study using the QTAIM analysis.

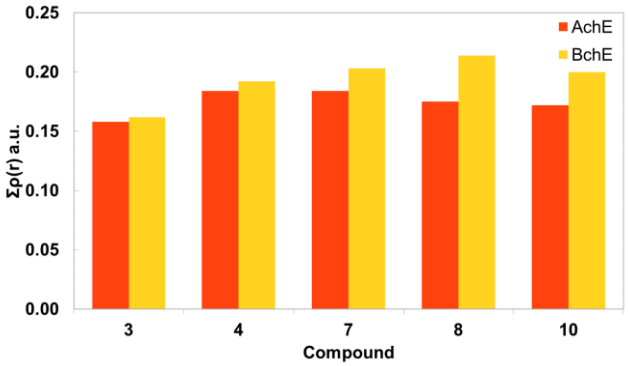

Figure 3. Sum of the values of charge density ($\sum\rho_{(r)}$) at the bond critical points obtained for the different compounds. The interactions are shown in orange for AChE and in yellow for BChE.

Compound **3** is bonded to the AchE through weak non classical hydrogen bond while in the BchE complex this inhibitor has the classical hydrogen bond well-oriented. The benzodioxole moiety act as H-Bond acceptor forming a non-classical hydrogen bond with Phe337, ($HE2_{Phe337,AChE}\bullet\bullet\bullet O_{Inh3}$) in the AChE complex, while in the BChE complex presents two moderate hydrogen bonds with Tyr332 ($HH_{Tyr332,BChE}\bullet\bullet\bullet O2_{Inh3}$) and Ty440 ($HH_{Tyr440,BChE}\bullet\bullet\bullet O1_{Inh4}$). Both complexes present a hydrogen bond with the carbonyl group with the residue Ser124 ($HG_{Ser124,AChE}\bullet\bullet\bullet O01_{Inh3}$) and Thr120 ($HG1_{Trp120,BChE}\bullet\bullet\bullet O01_{Inh3}$) in the AchE and BchE respectively. In addition, the compound **3** has several π-stacking interactions with Trp82 in the BChE complex (**Figure 4**).

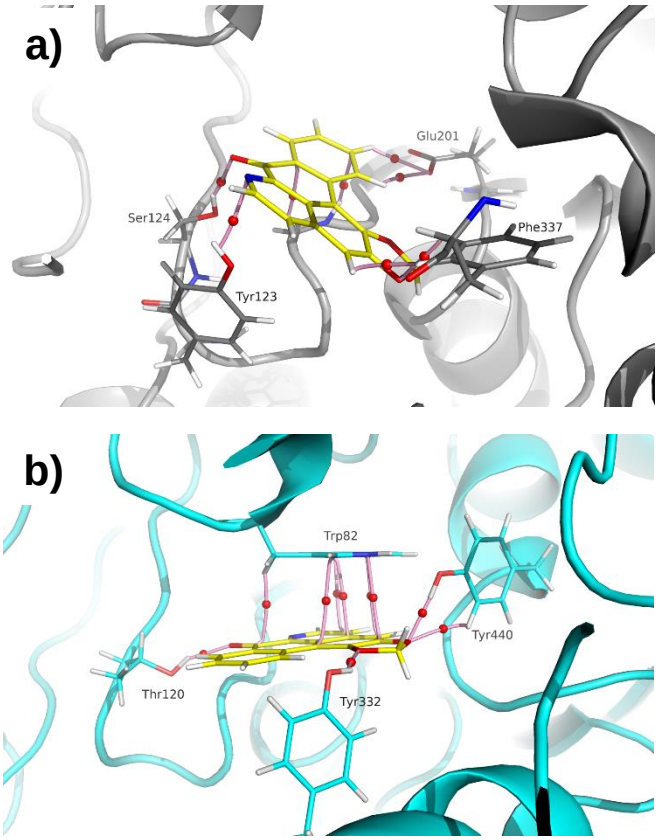

Figure 4. Molecular graph of the noncovalent interactions between compound **3** and (a) AChE and (b) BChE. The inhibitor is represented as yellow sticks while that the receptors are represented by grey and cyan cartoon, respectively. The elements of the electron density topology are shown. The bond paths connecting the nuclei are represented in pink sticks and the bond critical points are shown as red spheres.

Compound **4**, unlike compound **3** presents protonated nitrogen atom in the isoquinoline moiety and a methoxy group adjacent. In the AChE complex, these changes lead to the loss of the hydrogen bond with Ser124, while the quinoline nitrogen acts as H-bond donor against Tyr336 ($HO_{Tyr336,AChE}\bullet\bullet\bullet HN_{Inh4}$) (**Figure 5a**). On the contrary, in the BChE complex, the methoxide group forms a moderate hydrogen bond with Thr120 ($HG1_{Thr120,BChE}\bullet\bullet\bullet O01_{Inh4}$), while the quinoline nitrogen acts as a H-bon acceptor against amide group of Gly116 ($HN_{Gly116,BChE}\bullet\bullet\bullet N_{Inh4}$) (**Figure 5b**). The hydrophobic region of these compounds presents several contacts with Trp85 (AChE) and Trp82 (BChE), while that the compound **4** have two hydrogen bond weak with Glu201 in the AChE complex. The selectivity of this compound for BChE is mainly due to the strong anchoring provided by the hydrogen bonds that form the benzodioxole group with the Tyr332 ($HH_{Tyr332,BChE}\bullet\bullet\bullet O2_{Inh4}$) and Ty440 ($HH_{Tyr440,BChE}\bullet\bullet\bullet O1_{Inh4}$) while in the AChE complex this

group presents a moderate hydrogen bond with Ser202 ($HG_{Ser202,BChE}$•••$O1_{Inh4}$).

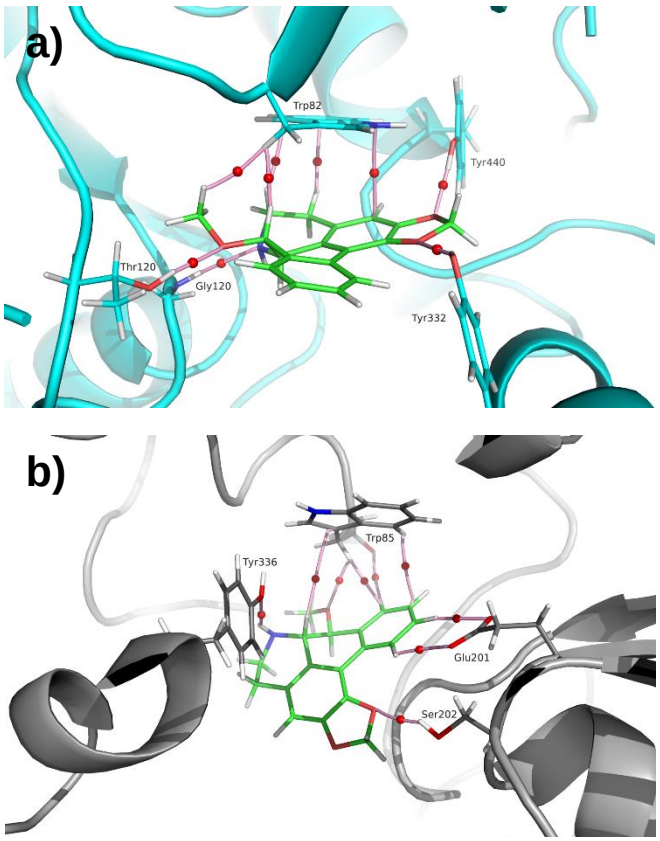

Figure 5. Molecular graph of the noncovalent interactions between compound **4** and (a) AChE and (b) BChE. The inhibitor is represented as green sticks while that the receptors are represented by grey and cyan cartoon, respectively.

The structural changes in compound **7**, respect to compounds **3** and **4**, render its inactivity against AChE, as shown in **Figure 6**, the interaction $HO_{Tyr336,AchE}$•••HN_{Inh7} that had compound **3** and **4** was lost by the incorporation of the methyl group. This moderate hydrogen bond was replaced by a very weak non-classical hydrogen bond ($HO_{Tyr336,AchE}$•••HC_{Inh7}). In addition, the breaking of the benzodioxole group causes the loss of the hydrogen bond with Ser202 ($HG_{Ser202,BChE}$•••$O1_{Inh4}$) present in compounds **4**, which is replaced by a non-classical hydrogen bond ($OG_{Ser202,BChE}$•••HC_{Inh7}). On the other hand, in the BChE complex, compound **7** retains the hydrogen bond with Thr120 ($HG1_{Thr120,BChE}$•••$O01_{Inh7}$) and Gly116 ($HN_{Gly116,BChE}$•••N_{Inh7}) as well as the hydrophobic contacts with Trp82. It is important to note that the breaking of the benzodioxole group causes the loss of the interaction with Tyr332 ($HH_{Tyr332,BChE}$•••$O2_{Inh7}$) , while the hydrogen bond with the OH group of Tyr440 ($HH_{Tyr440,BChE}$•••$O1_{Inh7}$) is a very important anchor point for the inhibitory activity of compound **7** and is key to the selectivity of this compound.

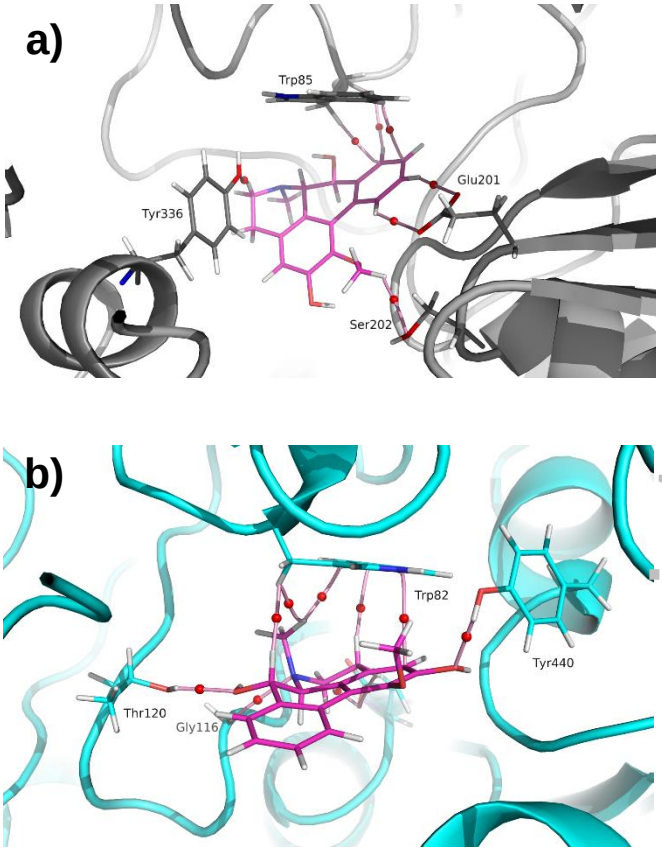

Figure 6. Molecular graph of the noncovalent interactions between compound **7** and (a) AChE and (b) BChE. The inhibitor is represented as magenta sticks while that the receptors are represented by grey and cyan cartoon, respectively.

In the AChE complex the compounds **8** and **10**, like compound **4** forms a hydrogen bond between the quinoline nitrogen and Tyr336 ($HO_{Tyr336,AChE}$•••$HN_{Inh8,10}$) while the hydrophobic contacts with Trp85 are conserved (**Figure 7a** and **Figure 8a**). On the other hand, the 11-methoxy substituent presents two non-classical hydrogen bond with Glu201 ($OE1_{Glu201,AChE}$•••$HC_{Inh8,10}$, $OE2_{Glu201,AChE}$•••$HC_{Inh8,10}$). It should be noted, that the small structural changes respect the other compounds generate a different mode of union in which valuable interactions such as those produced in compounds **3** and **4** between the benzodioxole group and Ser202 are missed. In contrast, in the BChE complex the isoquinoline region of compound **8** and **10** is strongly bounded by interactions with the Thr ($HG1_{Thr120,BChE}$•••$O01_{Inh8,10}$) and Gly ($HN_{Gly116,BChE}$•••$N_{Inh8,10}$) residues while the dioxolo moiety also participates in a large number of hydrophobic contacts with Thr82. Compounds **8** and **10** differ in the anchoring of the benzodioxole group. In compound **8** this group forms a hydrogen bond with Tyr440 ($HH_{Tyr440,BChE}$•••$O1_{Inh8}$) while in compound 10 it has two hydrogen bonds with Tyr 332 ($HH_{Tyr332,BChE}$•••$O2_{Inh10}$) and Tyr440 ($HH_{Tyr440,BChE}$•••$O1_{Inh10}$) (**Figure 7b** and **Figure 8b**).

It is important to note that the mode of union of these compounds is similar to that reported by other authors in many articles. In the case of AChE, it is reflected in the hydrogen bridge interactions with residues Tyr332 and Glu201 as well as with hydrophobic interactions with residues Trp85 and Phe337. On the other hand, in the case of BChE these compounds have important hydrogen bridge interactions with the Thr120, Tyr332 and Tyr440 residues while they have numerous hydrophobic interactions with the Trp82 residue. [27,28]

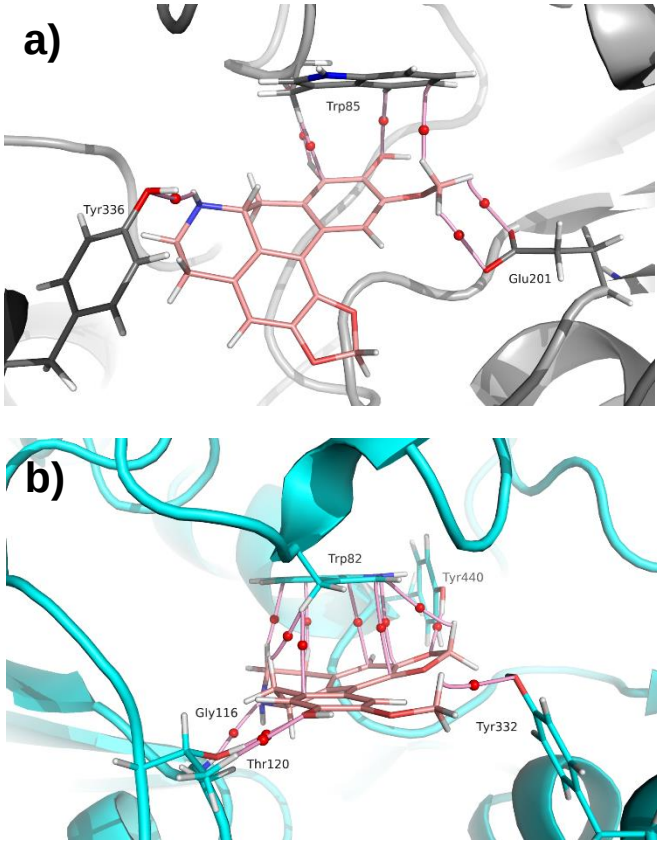

Figure 7. Molecular graph of the noncovalent interactions between compound **8** and (a) AChE and (b) BChE. The inhibitoris represented as orange sticks while that the receptors are represented by grey and cyan cartoon, respectively.

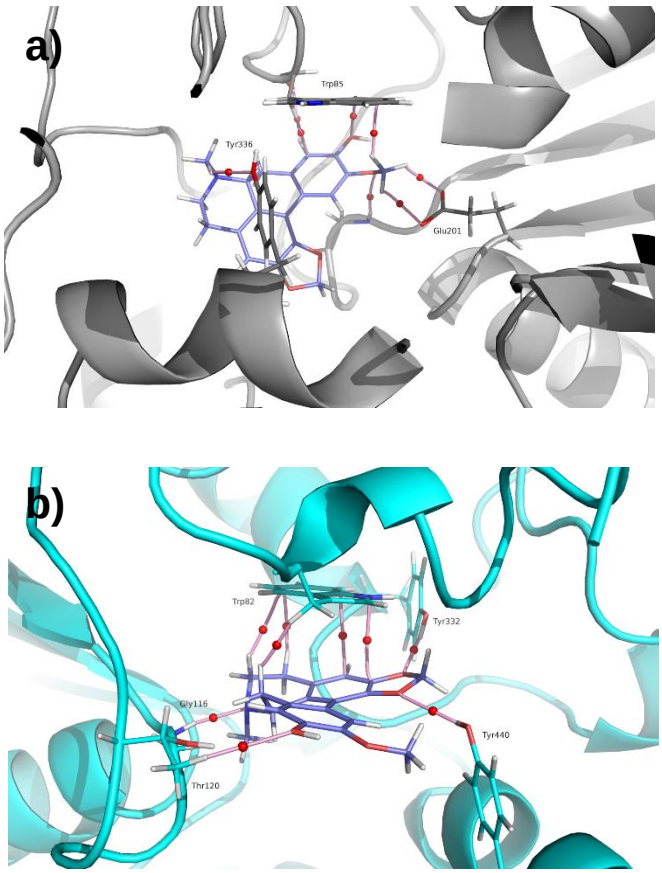

Figure 8. Molecular graph of the noncovalent interactions between compound 10 and (a) AChE and (b) BChE. The inhibitor is represented as light blue sticks while that the receptors are represented by grey and cyan cartoon, respectively.

4 Conclusions

In the current study, thirteen alkaloids of natural origin with aporphinoid structure were tested for their cholinesterase inhibitory activity. All of them were shown to interact with at least one of the enzymes. Alkaloids liriodenine **3** and cassythicine **10** demonstrated the best activity as dual inhibitors of AChE and BChE with IC_{50} values in the micromolar range. Also, these alkaloids were demonstrated to inhibit BChE more effectively than current drug for AD treatment galanthamine. In addition, molecular modelling analysis allowed us to explain the selectivity and mode of inhibition of some of the compounds trough the study of the interactions in the enzymes active sites. Benzodioxole moiety seemed to be responsible for the strong interaction between these subgroups of alkaloids and AChE and BChE.

Acknowledgements

This work was supported from UNSL (PROICO 02-2516), PICT 2017-0785 Pmo. BID and Alexander von Humboldt Foundation from Germany. These subsidies are gratefully acknowledged. The authors would like to thank Universidad Nacional de San Luis (UNSL), Universidad Nacional del Sur (UNS) (Argentina) and the Consejo Nacional de Investigaciones Científicas y Técnicas (CONICET). Finally,

authors want to thank language revision by staff of the Instituto de Lenguas of UNSL.

References

[1]. A. Kumar, A. Singh, and Ekavali, *Pharmacol. Reports* **2015**.
[2]. R. T. Bartus, Exp. Neurol. **2000**,163, 495-529.
[3]. C. N. Pope and S. Brimijoin, *Biochem. Pharmacol.* **2018**,153, 205-216.
[4]. P. Anand and B. Singh, Arch. *Pharm. Res.***2013**, 36, 375-399.
[5]. Q. Li, H. Yang, Y. Chen, and H. Sun, *Eur. J. Med. Chem.* **2017**, 132, 294-309.
[6]. V. K. Nuthakki, R. Mudududdla, A. Sharma, A. Kumar, and S. B. Bharate, *Bioorg. Chem.* **2019**.
[7]. C. Oliveira, D. Bagetta, F. Cagide, J. Teixeira, R. Amorim, T. Silva, J. Garrido, F. Remião, E. Uriarte, P. J. Oliveira, S. Alcaro, F. Ortuso, and F. Borges, *Eur. J. Med. Chem.* **2019**.
[8]. N. Di Marco, C. Lucero-Estrada, and C. R. Pungitore, *Lett. Appl. Microbiol.* **2019**.
[9]. C. Stévigny, C. Bailly, and J. Quetin-Leclercq, *Curr. Med. Chem. Anticancer. Agents*. **2005**, 5, 173-182.
[10]. S. K. Tripathi, T. Xu, Q. Feng, B. Avula, X. Shi, X. Pan, M. M. Mask, S. R. Baerson, M. R. Jacob, R. R. Ravu, S. I. Khan, X. C. Li, I. A. Khan, A. M. Clark, and A. K. Agarwal, *J. Biol. Chem.* **2017**.
[11]. A. Mollataghi, E. Coudiere, A. H. A. Hadi, M. R. Mukhtar, K. Awang, M. Litaudon, and A. Ata, *Fitoterapia*. **2012**, 83, 298-302.
[12]. Z. D. Yang, X. Zhang, J. Du, Z. J. Ma, F. Guo, S. Li, and X. J. Yao, *Nat. Prod. Res.* **2012**.
[13]. J. W. Dong, L. Cai, Y. S. Fang, H. Xiao, Z. J. Li, and Z. T. Ding, *Fitoterapia*. **2015**.
[14]. M. Leboeuf, A. Cavé, P. K. Bhaumik, B. Mukherjee, and R. Mukherjee, *Phytochemistry*. **1980**.
[15]. M. Nieto, T. Sevenet, M. Leboeuf, and A. Cave, *Planta Med.* **1976**.
[16]. G. L. Ellman, K. D. Courtney, V. Andres, and R. M. Featherstone, *Biochem. Pharmacol.* **1961**.
[17]. G. M. Morris, R. Huey, W. Lindstrom, M. F. Sanner, R. K. Belew, D. S. Goodsell, and A. J. Olson, *J. Comput. Chem.* **2009**, 30, 2785-2791.
[18]. D.A. Case, I.Y. Ben-Shalom, S.R. Brozell, D.S. Cerutti, T.E. Cheatham, III, V.W.D. Cruzeiro, T.A. Darden, R.E. Duke, D. Ghoreishi, M.K. Gilson, H. Gohlke, A.W. Goetz, D. Greene, R Harris, N. Homeyer, S. Izadi, A. Kovalenko, T. Kurtzman, T.S. Lee, S. LeGrand, P. Li, C. Lin, J. Liu, T. Luchko, R. Luo, D.J. Mermelstein, K.M. Merz, Y. Miao, G. Monard, C. Nguyen, H. Nguyen, I. Omelyan, A. Onufriev, F. Pan, R. Qi, D.R. Roe, A. Roitberg, C. Sagui, S. Schott-Verdugo, J. Shen, C.L. Simmerling, J. Smith, R. Salomon-Ferrer, J. Swails, R.C. Walker, J. Wang, H. Wei, R.M. Wolf, X. Wu, L. Xiao, D.M. York and P.A. Kollman (2016), AMBER 2016, University of California, San Francisco.
[19]. X. Guo, D. He, L. Huang, L. Liu, L. Liu, and H. Yang, *Comput. Theor. Chem.* **2012**.
[20]. J. Wang, R. M. Wolf, J. W. Caldwell, P. A. Kollman, and D. A. Case, *J. Comput. Chem.* **2004**, 25, 1157-1174.
[21]. Gaussian 16, Revision C.01, M. J. Frisch, G. W. Trucks, H. B. Schlegel, G. E. Scuseria, M. A. Robb, J. R. Cheeseman, G. Scalmani, V. Barone, G. A. Petersson, H. Nakatsuji, X. Li, M. Caricato, A. V. Marenich, J. Bloino, B. G. Janesko, R. Gomperts, B. Mennucci, H. P. Hratchian, J. V. Ortiz, A. F. Izmaylov, J. L. Sonnenberg, D. Williams-Young, F. Ding, F. Lipparini, F. Egidi, J. Goings, B. Peng, A. Petrone, T. Henderson, D. Ranasinghe, V. G. Zakrzewski, J. Gao, N. Rega, G. Zheng, W. Liang, M. Hada, M. Ehara, K. Toyota, R. Fukuda, J. Hasegawa, M. Ishida, T. Nakajima, Y. Honda, O. Kitao, H. Nakai, T. Vreven, K. Throssell, J. A. Montgomery, Jr., J. E. Peralta, F. Ogliaro, M. J. Bearpark, J. J. Heyd, E. N. Brothers, K. N. Kudin, V. N. Staroverov, T. A. Keith, R. Kobayashi, J. Normand, K. Raghavachari, A. P. Rendell, J. C. Burant, S. S. Iyengar, J. Tomasi, M. Cossi, J. M. Millam, M. Klene, C. Adamo, R. Cammi, J. W. Ochterski, R. L. Martin, K. Morokuma, O. Farkas, J. B. Foresman, and D. J. Fox, Gaussian, Inc., Wallingford CT, 2016. and D. J. F. M. J. Frisch, G. W. Trucks, H. B. Schlegel, G. E. Scuseria, M. A. Robb, J. R. Cheeseman, G. Scalmani, V. Barone, G. A. Petersson, H. Nakatsuji, X. Li, M. Caricato, A. V. Marenich, J. Bloino, B. G. Janesko, R. Gomperts, B. Mennucci, H. P. Hratchian, J. V., (2016).
[22]. R. F. W. Bader, *Acc. Chem. Res.* **1985**, 18, 9-15.
[23]. T. Lu and F. Chen, *J. Comput. Chem.* **2012**, 33, 580-592.
[24]. J.-W. Dong, L. Cai, X.-J. Li, J.-P. Wang, R.-F. Mei, and Z.-T. Ding, *Arch. Pharm. Res.* **2017**, 40, 1394-1402.
[25]. J. Cheung, M.J. Rudolph, F. Burshteyn, M.S. Cassidy, E.N. Gary, J. Love, M.C. Franklin and J.J. Height, *J. Med. Chem.* **2012**, 22, 10282-10286
[26]. F. Nachon, E. Carletti, C. Ronco, M. Trovaslet, Y. Nicolet, L. Jean and P.Y. Renard, *Biochem J.* **2013**, 453,393-399.
[27]. M.T. Khan, I. Orhan, F.S. Senol, M. Kartal, B. Sener, M. Dvorská, K. Smejkal and T. Slapetová, *Chem Biol Interact.* **2009**, 181, 383-389
[28]. G.L. Delogu, M.J. Matos, M. Fanti, B. Era, R. Medda, E. Pieroni, A. Fais, A. Kumar and F. Pintus, *Bioorg Med Chem Lett.* **2016**, 26, 2308-2313.

Received: ((will be filled in by the editorial staff))
Accepted: ((will be filled in by the editorial staff))
Published online: ((will be filled in by the editorial staff))

10.1002/minf.201900125